



*Cent. Eur. J. Energ. Mater.* 2024, 21(3): 235-254; DOI 10.22211/cejem/193815

Article is available in PDF-format, in colour, at:

<https://ipo.lukasiewicz.gov.pl/wydawnictwa/cejem-woluminy/vol-21-nr-3/>



Article is available under the Creative Commons Attribution-NonCommercial-NoDerivs 3.0 license CC BY-NC-ND 3.0.

*Research paper*

## Integrating Moisture Isotherms, Compatibility Assessment, and Model Propellant with ADN as an Eco-Friendly Oxidizer

Deepak Yadav, Kavita Ghosh\*), Vaibhav Sadavarte, Lalita Jawale, Rajesh BabanRao Pawar, Ramesh Kurva  
*High Energy Materials Research Laboratory (HEMRL), Pune – 411 021, India*

\* *E-mail:* [ghosh.kavita.hemrl@gov.in](mailto:ghosh.kavita.hemrl@gov.in)

### ORCID Information

Deepak Yadav: <https://orcid.org/0009-0007-1711-6260>

Kavita Ghosh: <https://orcid.org/0000-0002-9158-8633>

Vaibhav Sadavarte: <https://orcid.org/0000-0003-1409-6691>

**Abstract:** This study delves into the use of ammonium dinitramide (ADN) as an eco-friendly substitute for ammonium perchlorate (AP) in solid rocket propellants. ADN based novel propellants were formulated with a nitrile butadiene rubber (NBR) based binder system. Employing Dynamic Vapor Sorption (DVS), ADN's moisture characteristics were investigated at various temperatures (25, 35, 45 and 55°C) and utilized for propellant processing. Two component chemical compatibility assessments, in adherence to STANAG 4147 standard, were performed using Differential Scanning Calorimetry (DSC) and Vacuum Stability Testing (VST). Subsequently, propellant compositions containing ADN were formulated, and their performance was predicted using NASA's CEC-71 code. The most promising formulation was processed and thereafter underwent testing for physical, ballistic, and mechanical performance against conventional AP-based propellants at a 500 g batch level. Optimal storage ( $\leq 25$  °C, relative humidity (RH)  $\leq 50\%$ ) and processing (35-40 °C, RH  $\leq 35\%$ ) performance conditions were identified for ADN, contributing to the successful formulation of high-performance ADN/NBR propellant. The developed propellant showed

marginal differences compared to AP/NBR in burn rate and density. However, compatibility issues with the bonding agent, hydantoin resin, led to deficiencies in mechanical strength. These findings contribute to the advancement of eco-friendly propellant technology, showcasing ADN's potential as a transformative substance in aerospace applications.

**Keywords:** ammonium dinitramide, ADN, RDX, quinol ether, propellant, Dynamic Vapor Sorption, DVS, compatibility

## 1 Introduction

Solid rocket propellants play a pivotal role in the expansive field of aerospace technology, providing the necessary thrust for unmanned aerial vehicles (UAVs) [1], missiles, and rockets [2-4]. Recognized for their unwavering reliability, rapid ignition capabilities, and exceptional effectiveness in critical missions, solid rocket propellants underscore their irreplaceable significance in modern propulsion technologies. Among the diverse array of solid rocket propellants, the AP/aluminum composite propellants, utilizing hydroxyl-terminated polybutadiene (HTPB) as a binder, have gained prominence through widespread adoption [5]. The components constituting these AP-based composites have undergone exhaustive research efforts [6] and adaptability across a variety of climatic conditions worldwide. However, their cost-effectiveness and good performance come with concerns about the environment and toxicity, which have gained a lot of attention [7-11]. This environmental challenge revolves around perchlorate contamination, reaching a global scale and necessitating collaborative efforts from nations worldwide to address the escalating concerns [12, 13].

Against the backdrop of growing environmental concerns, ADN emerges as a promising alternative to AP [14]. ADN presents a range of compelling advantages, notably breaking away from chlorine-rich combustion byproducts [15]. This departure simplifies water extraction and demilitarization processes, resulting in cleaner emissions and an enhanced energy yield [15, 16]. However, the adoption of ADN comes with its unique set of challenges, including a propensity for agglomeration [17], pronounced hygroscopicity [18, 19], and incompatibility with specific rocket propellant ingredients [20]. The significant hygroscopic nature of ADN has broad implications, affecting its storage, compromising safety, destabilizing thermal properties, accelerating degradation, compromising mechanical integrity, and ultimately reducing overall propellant performance [21, 22]. Consequently, it becomes imperative to store ADN within an environment that maintains a RH below 55% [23].

Dynamic Vapor Sorption (DVS) has emerged as an indispensable technique, providing real-time and precise measurements of moisture sorption through controlled vapor concentration variations around the sample and subsequent measurement of its changing mass over time [24]. This method stands as a pivotal gravimetric tool, demonstrating remarkable versatility across a wide humidity range, surpassing the efficiency and sensitivity of traditional salt methods [25, 26]. In a noteworthy study, Wang effectively illustrates the advantages of the DVS method over traditional salt-based techniques, using ADN as a case in point [27]. The apparatus involved in this method includes a precisely controlled incubator housing a microbalance, sample and reference chambers, alongside temperature and humidity probes, ensuring meticulous measurements. A schematic representation illustrating the functioning of DVS is presented in Figure 1. To comprehensively investigate how moisture influences ADN, we conducted an extensive assessment covering a broad humidity range, from 0% to 90% RH, and determined the effect at four different temperatures: 25, 35, 45 and 55 °C.

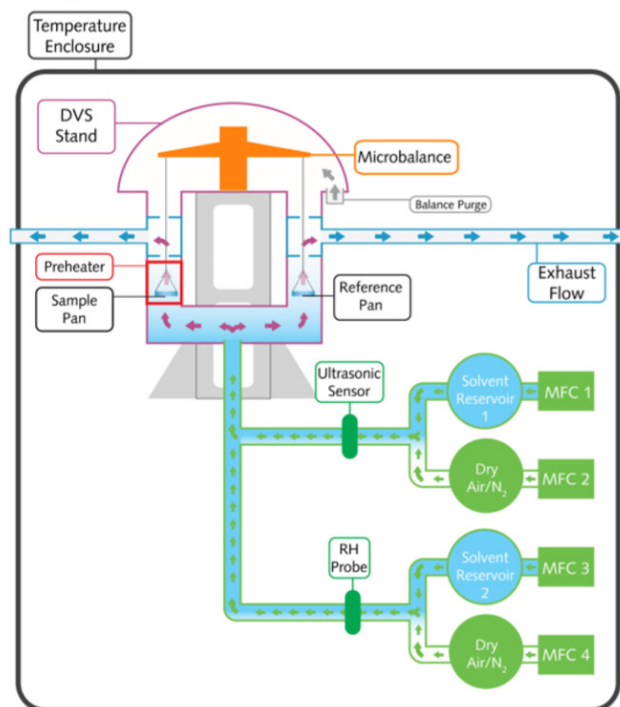


**Figure 1.** Schematic of the DVS instrument showing direction of carrier gas flow (solid arrows) (© Surface Measurements System)

The data obtained from DVS experiments was used to identify the optimal conditions for processing ADN-based propellants, specifically focusing on humidity and temperature settings. Once the ADN storage and processing conditions were determined, we proceeded with formulating the propellant. Considering ADN's incompatibility with isocyanates [28], a quinol ether (4,4'-((cyclohexa-2,5-diene-1,4-diylidene)bis(azanylydene))bis((oxy))bis(2,4,6-tri-tert-butylcyclohexa-2,5-dienone) based curing system was chosen for propellant formulations. However, the literature reports various binder systems, such as GAP and triazole systems, for use with ADN [29-32]. For this research, an established binder system comprising NBR and triethyleneglycol dinitrate (TEGDN) cured with quinol ether of 1,4-benzoquinone dioxime was preferred. This choice offers advantages, including reduced toxicity and sensitivity, and enhanced resistance to moisture-related issues compared to isocyanates. The science behind quinol ether of 1,4-benzoquinone dioxime based curing involves a distinctive reaction where the dinitrosobenzene in quinol ether engages with NBR, resembling a pseudo Diels-Alder reaction [33]. Sudhir *et al.* [34] demonstrated the effectiveness of this quinol ether based curing in AP/aluminium-based formulations.

To ensure the safety and reliability of the ADN/NBR propellant, an extensive examination of chemical compatibility between ADN and propellant ingredients was carried out. This assessment was conducted through precise methods, including DSC and VST, following the guidelines outlined in North Atlantic Treaty Organization (NATO) standardization agreement (STANAG) 4147 [35]. Once compatibility was established, the theoretical performance of ADN-based propellants concerning thermo-chemical properties was evaluated using the NASA CEC-71 code. Based on the theoretical performance predictions, a 500 g batch was processed, and various physical, ballistic, and mechanical properties were determined after successful curing. Comparing ADN-based and AP-based formulations – both theoretically and practically, provided valuable insights into ADN's behavior in solid rocket propellants. This research showcases ADN/NBR potential in developing eco-friendly propellants, contributing to aerospace technology's advancement and environmental sustainability.

## 2 Materials and Methods

### 2.1 Materials

The materials used in this study were obtained as follows: Prilled ADN (purity >95%) was sourced from JSC ROSO Boron Export, Russia. AP, with an average

particle size of  $300 \pm 10 \mu\text{m}$ , was procured from M/s Pandian Chemicals Ltd. (Cuddalore, India) and further ground to a particle size of approximately  $50 \pm 2 \mu\text{m}$  using an air classifier mill for bimodal AP. Aluminum powder, with an average particle size of  $6 \pm 1 \mu\text{m}$ , was obtained from the Metal Powder Company, Madurai, and used as received. RS-RDX was supplied by M/s Solar Industries India Ltd. (India). The solid cure catalyst, lead oxide, was sourced from trade. TEGDN was procured from Bharat Explosives Ltd. (Lalitpur, India). NBR was obtained from Abhang Organics (Pune, India), and quinol ether was sourced from Indian Adhesives and Glues (Pune, India). TEGDN and NBR were mixed to form the active binder. Hydantoin resin was procured from M/s Indian Adhesives and Glues (Pune, India).

## 2.2 Analysis methods

Dynamic Vapor Sorption (DVS) measurements were conducted on Surface Measurement Systems DVS Resolution 1. The experiments were conducted in  $\text{dm}/\text{dt}$  mode (% change in mass per minute) with 180 min as the maximum equilibration time serving as the stage-end determination criterion. If the sample achieved equilibrium, it would move to the next stage of RH. However, if the time limit of 180 min was reached without achieving equilibrium, the DVS would still proceed to the next RH stage. To comprehensively evaluate the influence of relative humidity on ADN, a method was devised with stepwise changes in humidity levels, ranging from 0% to 90% RH. Considering ADN's inherent hygroscopic nature, approximately 25 mg of ADN was employed to achieve a more reliable signal-to-noise ratio during measurements. A threshold  $\text{dm}/\text{dt}$  value of 0.002% was set as the condition for the sample to reach equilibrium before concluding each stage.

Fourier Transform Infrared Spectroscopy (FTIR) spectra were recorded on a Perkin Elmer Sr. No. 1118562 spectrometer employing Attenuated Total Reflectance (ATR).

Differential Scanning Calorimetry (DSC) measurements were performed using a TA DSCQ20 with RCS 90 as cooling accessory. The measuring cell was purged with nitrogen ( $50 \text{ mL} \cdot \text{min}^{-1}$ ). The samples were first dried as per the specification. Moisture content was below 0.1% and volatile matter (aluminum and lead dioxide) was below 0.05%. The samples were placed in hermetically sealed pinhole aluminum pans and heated at a temperature between 50 and 300 °C. For ADN and ADN after DVS, approximately  $1 \pm 0.01 \text{ mg}$  sample was analyzed at a heating rate of  $10 \text{ }^\circ\text{C} \cdot \text{min}^{-1}$ . Melting point and decomposition temperature was determined based on peak temperature. For chemical compatibility  $1 \pm 0.1 \text{ mg}$  of pure compounds and  $2 \pm 0.01 \text{ mg}$  of mixtures (1:1 ratio) were

analyzed at a heating rate of  $2\text{ }^{\circ}\text{C}\cdot\text{min}^{-1}$ . For analysis, a peak shift below  $4\text{ }^{\circ}\text{C}$  was considered as compatible, while shifts between  $4$  and  $20\text{ }^{\circ}\text{C}$  hinted a small degree of incompatibility. Shifts exceeding  $20\text{ }^{\circ}\text{C}$  were considered entirely incompatible as per STANAG 4147 [35]. The temperature was adjusted using calibration with indium.

Vacuum stability tests (VST) were conducted using a Vacuum Stability Tester, OZM Stabil 21 VST model. Both pure substances and mixtures (mass ratio: 1:1) were analyzed for their gas evolution behavior. Approximately  $2.5 \pm 0.01\text{ g}$  of pure materials and  $5 \pm 0.01\text{ g}$  of 1:1 mixtures were placed in glass test tubes and exposed to a time-temperature load for duration of 40 h at  $80\text{ }^{\circ}\text{C}$ . For analysis, if the mixture showed an additional gas generation of  $5\text{ cm}^3$  compared to the respective test material, then the test material was deemed incompatible. For VST studies, the temperature was set at  $80\text{ }^{\circ}\text{C}$  due to ADN's low melting point [36].

Automatic explosion temperature (AET) measurements were performed using an Automatic Explosion Temperature Tester, OZM AET 402. A 50 mg sample was heated at a controlled rate of  $5\text{ }^{\circ}\text{C}\cdot\text{min}^{-1}$  in a test tube until an explosion occurred. The temperature at which the explosion happened was recorded as the explosion temperature.

A Pycnometric EVO helium gas pycnometer (Thermo Scientific) was employed to ascertain the density of the propellant samples. Each sample was cut into pieces measuring  $25 \times 25 \times 25\text{ mm}$  and was subsequently filled to 60-70% volume within the sample vessel. The sample vessel was then positioned in the instrument's sample chamber, and the density of the sample was measured.

Mechanical properties, including tensile strength (TS), E-modulus (E-mod), and percent elongation (%E), were determined using a Hounsfield Universal Testing Machine (UTM) following ASTM-D-638 type IV standards. Tests were conducted at a cross head speed of  $50\text{ mm}\cdot\text{min}^{-1}$  at ambient temperature. Specimens, with measured width and thickness, were aligned in the machine grips and stretched. Load/extension curves were recorded to derive TS, %E, and E-mod values. Strain was measured by determining the extension of propellant strands at maximum stress, with an initial gauge length of 45 mm.

The burn rate of the cured composite solid propellant samples was determined using the acoustic emission technique under an inert nitrogen atmosphere at 7 MPa within a  $750\text{ cm}^3$  stainless steel bomb. The bomb was equipped with a lid featuring a panel for securing the propellant strand and a piezoelectric transducer. The propellant samples, shaped as strands with dimensions of  $150 \times 6 \times 6\text{ mm}$ , were ignited from one end using a nichrome wire. Manual measurement errors may result in an expected accuracy of  $\pm 0.5\text{ mm}\cdot\text{s}^{-1}$  in the measured burn rate.

### 2.3 Propellant processing

All the experiments were carried out at 500 g batch level in a three blade vertical planetary mixer equipped with a water jacketed bowl. A general method for preparation of propellant composition is as follows. Firstly, all binder ingredients were mixed and the active binder (NBR + TEGDN) was prepared and degassed for 30 min. Then solids were added sequentially by allowing finer to coarser particle size. After complete addition of solids, slurry was mixed for 60 min without vacuum and 60 min with vacuum for homogenization. Processing temperature of the slurry was maintained around 35-40 °C at 35% RH. At this stage, a curative (quinol ether of 1,4-benzoquinone dioxime) was added by maintaining the temperature at 40 °C and mixed for 60 min. This slurry was cast under vacuum and cured at 50 °C for 20 days under pressure.

## 3 Results and Discussions

### 3.1 Sorption studies

DVS was employed to assess the moisture uptake and loss characteristics of ADN under varying RH conditions. Figure 2 illustrates the target and measured RH levels during the experiments. Additionally, the experiments were conducted at four distinct temperatures: 25, 35, 45 and 55 °C, to investigate the interplay between temperature and RH on ADN's behavior. This comprehensive DVS approach yielded valuable insights into how varying relative humidity and temperature conditions affects ADN's moisture sorption behavior. The subsequent sections will delve into the results obtained, discussing the implication for storage, processing, and overall applicability of ADN in solid rocket propellants formulations.

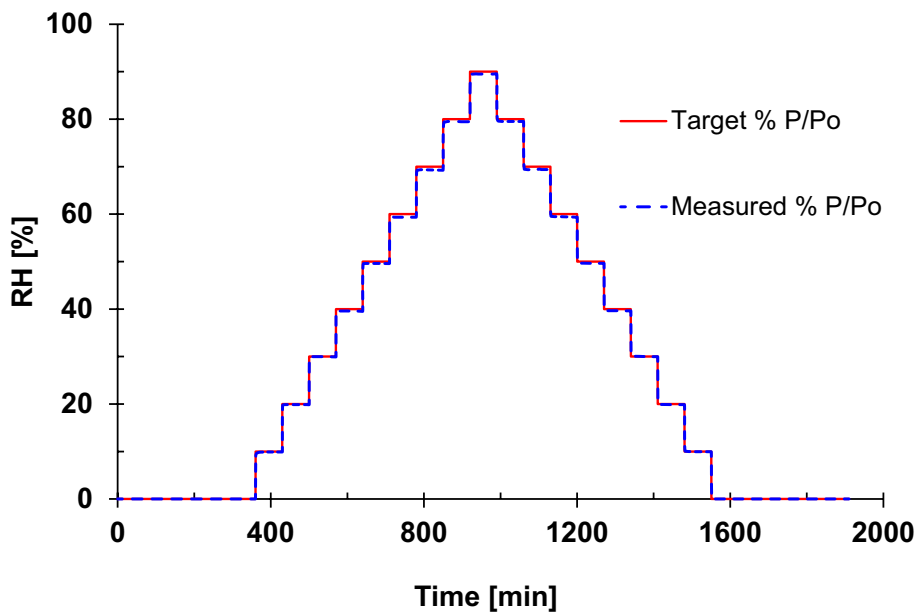


Figure 2. DVS graph illustrating target and measured RH

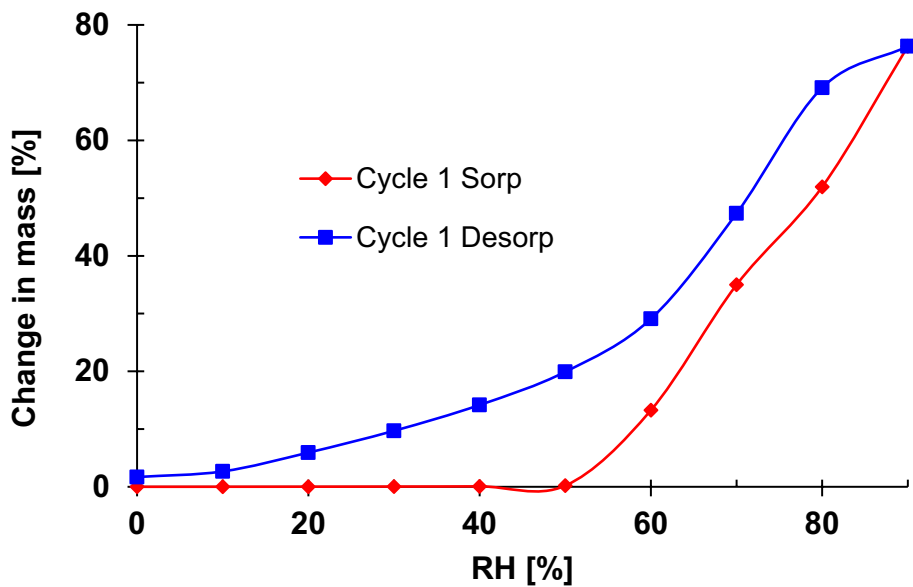
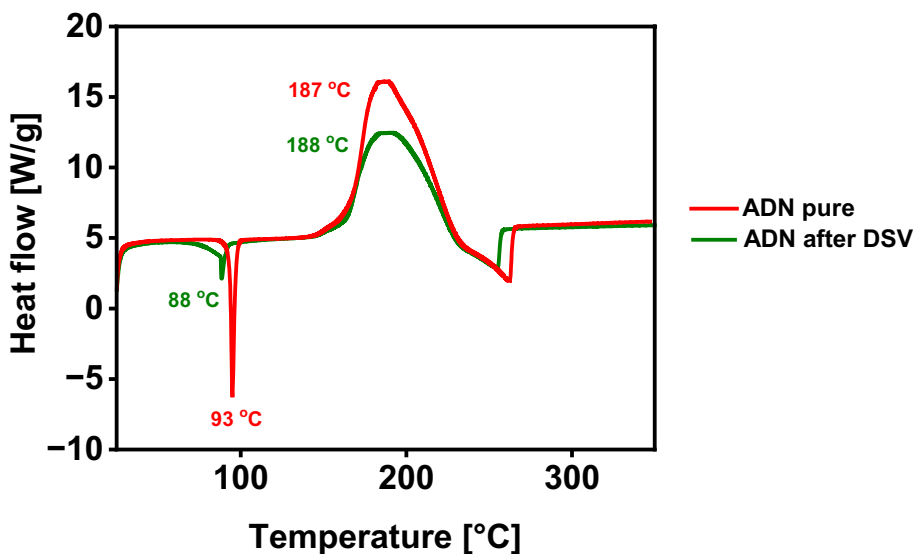


Figure 3. Sorption and desorption isotherms of pure ADN at 25 °C



The complete sorption/desorption isotherm at 25 °C, obtained from DVS is depicted in Figure 3. However, complete equilibrium (defined as a change in mass below 0.002% per unit time) was not achieved at RH levels of 60%, 70%, 80%, and 90% within the 180-min time limit at 25 °C. Notably, a sharp increase in moisture uptake is observed above the 50% RH mark, a characteristic feature of ADN's hygroscopic behavior. Specifically, at 50% RH, ADN displayed a maximum moisture uptake of only 0.15%. Conversely, at lower RH levels of  $\approx 30\%$  and  $\approx 40\%$ , the moisture uptake was substantially lower, 0.03% and 0.05%, respectively. Therefore, for the storage of ADN at 25 °C, the surrounding environment must be strictly controlled below 50% RH in order to keep moisture sorption minimum. The deliquescence point was noted between 50-60% RH. During desorption at 0% RH, prilled ADN was found to be converted into crystalline needle-shaped ADN. DSC and FTIR studies were conducted on ADN, both before and after the DVS experiments. The DSC analysis demonstrated a decrease in the melting at 88 °C, compared to 93 °C for pure ADN. The decomposition peak temperature of ADN after DVS was comparable to pure ADN. The observed change in the melting temperature can be attributed to the residual moisture which remained in ADN even after drying at 0% RH. A similar shift in melting temperature is reported in the literature between 5% RH ADN and pure ADN [19]. The overlay of DSC curves of pure ADN and ADN after DVS is given in Figure 4. The FTIR spectra of ADN, after DVS exposure shows an additional O–H vibration peak in the 3300  $\text{cm}^{-1}$  region, indicating the presence of newly formed hydrogen bonds resulting from moisture interaction. Figure 5 presents the comparison of FTIR studies of ADN and ADN after DVS. These findings provide critical insights into ADN's moisture sorption behavior and its subsequent impact on the thermal properties.



**Figure 4.** Overlay of DSC curves at the heating rate of  $10\text{ }^{\circ}\text{C}\cdot\text{min}^{-1}$  of pure ADN (red) and ADN after DVS at  $25\text{ }^{\circ}\text{C}$  (green)

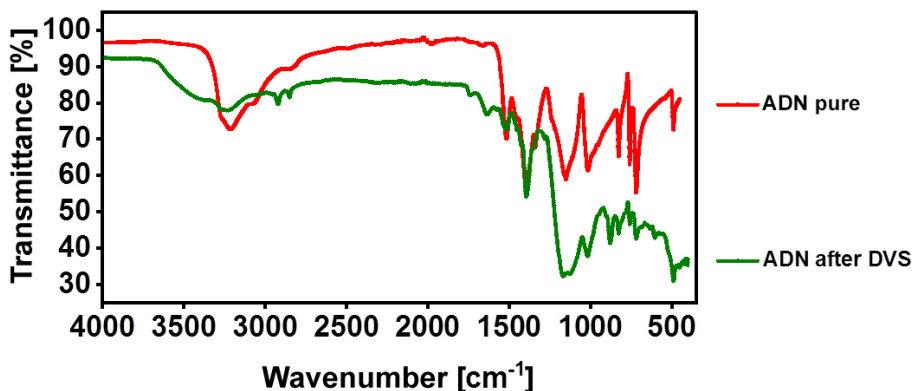


**Figure 5.** Overlay of FTIR curves of pure ADN (red) and ADN after DVS at  $25\text{ }^{\circ}\text{C}$  (green)

At elevated temperatures, it becomes evident that ADN displayed an increased rate of moisture absorption. Figure 6 presents the sorption curves, highlighting the effect of temperature variations at  $25$ ,  $35$ ,  $45$  and  $55\text{ }^{\circ}\text{C}$ . Notably, at  $55\text{ }^{\circ}\text{C}$ , the sharp upturn in moisture uptake commenced at a lower relative humidity ( $\approx 20\%$  RH) compared to  $45\text{ }^{\circ}\text{C}$  ( $\approx 30\%$  RH) and  $35\text{ }^{\circ}\text{C}$  ( $\approx 40\%$  RH).

From the data, it is evident that ADN must be stored under controlled conditions, maintaining relative humidity below 50% at 25 °C to mitigate moisture absorption. Conversely, for the ease of processing purposes, the most favorable conditions are achieved at 40 °C or below, with a relative humidity of  $\leq 35\%$ . It's important to note that higher temperatures exacerbate moisture absorption, and stricter humidity control is necessary for safe rocket motor processing, as increased sensitivity to moisture can deteriorate the quality of propellant. This comprehensive analysis of the impact of temperature and humidity on ADN's moisture sorption behavior is instrumental in defining the best practices for the storage and processing of ADN-based solid rocket propellants.

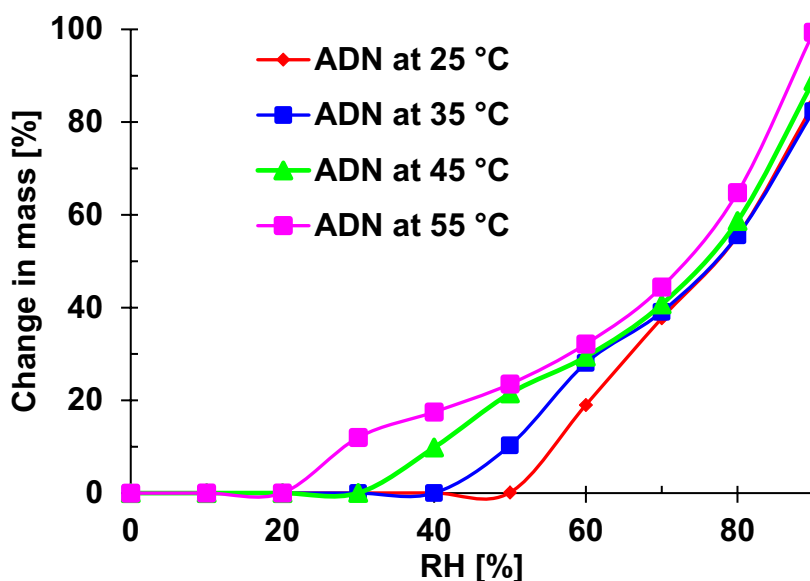


**Figure 6.** Overlay of sorption curves of ADN using DVS: ADN at 25 °C (red,  $\blacklozenge$ ), ADN at 35 °C (blue,  $\blacksquare$ ), ADN at 45 °C (green,  $\blacktriangle$ ) and ADN at 55 °C (pink,  $\blacksquare$ )

### 3.2 Compatibility

Prior to propellant processing, studies on the chemical compatibility of two components were conducted to assess ADN's compatibility with various solid rocket propellant ingredients, following the STANAG 4147. The propellant ingredients used for compatibility included hydantoin resin (1,3-diglycidyl-5,5-dimethylhydantoin) as bonding agent, active binder (NBR + TEGDN), quinol ether 1,4-benzoquinone dioxime as curing agent, AP, RS-RDX, aluminum,

and lead dioxide. To ensure the accuracy of the results, an initial assessment involved analyzing samples for moisture content and volatile matter. Only well dried samples that met the criteria of specified moisture content were selected for compatibility analysis. Additionally, the mixtures were analyzed for Auto Explosion Temperature (AET) to determine critical safety parameters. The results of the compatibility assessments, encompassing all relevant data, are presented in Table 1.

**Table 1.** Compatibility studies of ADN with solid rocket propellant ingredients

Mixture	$T_d$ [°C] (DSC method)	Volume of gas evolved using VST [ml]	AET [°C]	Compatible (C)/ Incompatible (IC)
ADN	172	E = 0.212	159	–
ADN + hydantoin resin	115 $\Delta T_d = 57$	Failed	170	IC
ADN + (NBR + TEGDN)	170 $\Delta T_d = 2$	S = 3.871 M = 4.413 $V_R = 0.330$	161	C
ADN + quinol ether	156/175 $\Delta T_d = -3$	S = 0.183 M = 0.507 $V_R = 0.112$	164	C
ADN + AP	172 $\Delta T_d = 0$	S = 0.182 M = 0.493 $V_R = 0.099$	165	C
ADN + RS-RDX	180 $\Delta T_d = -8$	S = 0.321 M = 0.710 $V_R = 0.177$	157	C
ADN + aluminum	169 $\Delta T_d = 3$	S = 0.085 M = 0.417 $V_R = 0.120$	168	C
ADN + PbO <sub>2</sub>	162 $\Delta T_d = 10$	S = 1.610 M = 1.928 $V_R = 0.106$	180	C

$T_d$  = exothermic peak of mixtures,  $\Delta T_d$  = exothermic peak of ADN minus exothermic peak of mixtures; E = volume of gas from 2.5 g of ADN, S = volume of gas from 2.5 g of test material, M = volume of gas evolved from 5 g of mixture,  $V_R = M - (E + S)$

The decomposition temperature ( $T_d$ ) of pure ADN was determined to be 172 °C using the maximum temperature of the exothermic peak in DSC (heating rate of 2 °C·min<sup>-1</sup>). For the individual components, the pure decomposition peaks were observed at 167 °C for quinol ether, 259 °C for AP, and 225 °C for

RS-RDX. The mixture analysis revealed that ADN exhibited incompatibility with hydantoin resin. There was also some degree of incompatibility observed with quinol ether and lead dioxide. As per STANAG 4147, additional techniques need to be employed to further evaluate and confirm compatibility in these cases. On the other hand, ADN demonstrated good compatibility with active binder (NBR + TEGDN), AP, RS-RDX and aluminum using DSC. This conclusion was drawn from the observation that the decomposition peak of the mixture either met the 4 °C criteria stipulated by STANAG 4147 or exceeded the decomposition temperature of pure ADN. The DSC curves for the pure compounds and mixture are provided in Figures 8 and 9, respectively.

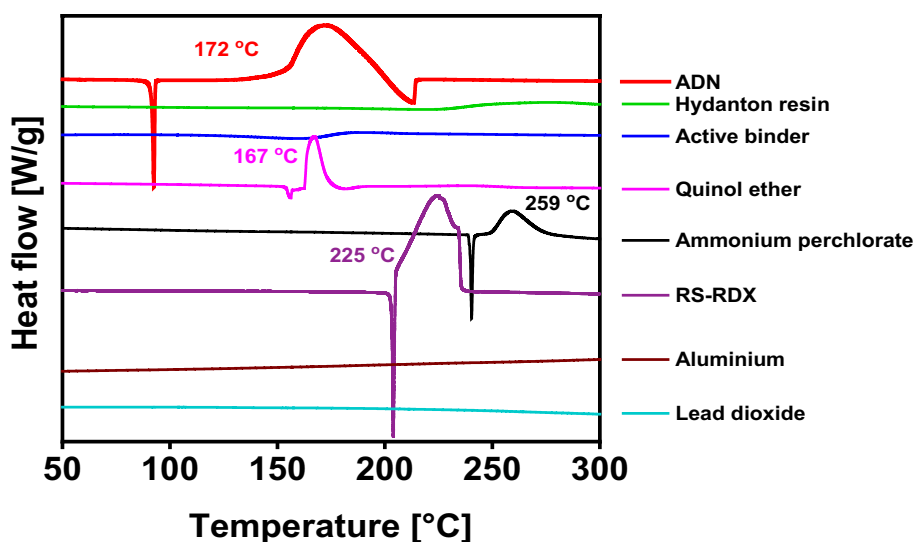


**Figure 8.** Overlay of DSC curves at heating rate of  $2\text{ °C}\cdot\text{min}^{-1}$  of pure ADN and other ingredients in their pure forms

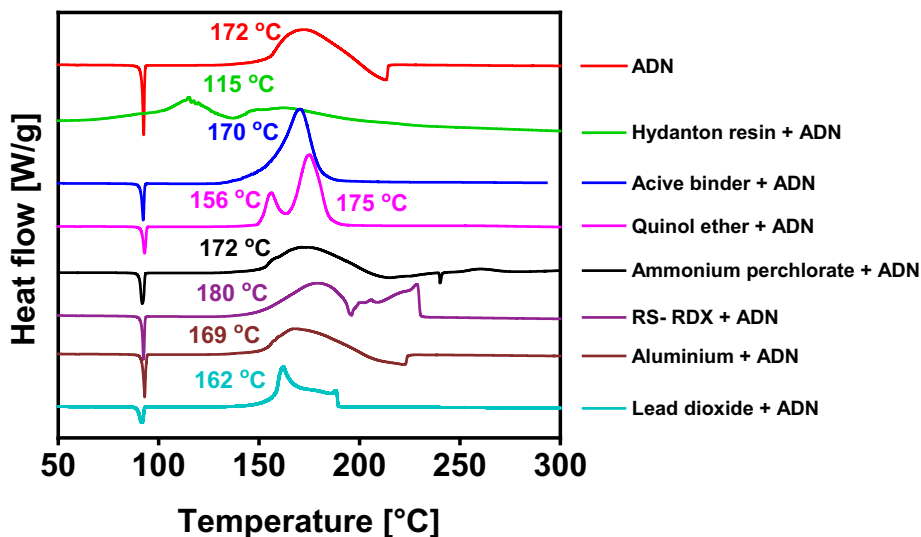


**Figure 9.** Overlay of DSC curves at heating rate of  $2\text{ }^{\circ}\text{C}\cdot\text{min}^{-1}$  for 1:1 mixtures of ingredients with ADN

For VST analysis, only solid test materials were examined in both their pure form and as mixtures with ADN. In the case of liquid test materials, only mixtures were evaluated. Bonding agents are typically used to interact with the surface of fillers to improve adhesion between fillers and binders [37]. The test for the combination of ADN and hydantoin resin, which is used as a bonding agent, failed due to a sudden exothermic reaction while exposing the test tube at  $80\text{ }^{\circ}\text{C}$ , indicating a failure in the compatibility test. This mixture also displayed incompatibility through DSC. Conversely, all other test materials demonstrated compatibility when accessed *via* VST. The volume ratio ( $V_R$ ), representing the volume of gas produced as a result of the reaction between components in the test mixture is detailed in Table 1.

### 3.3 Theoretical performance of propellant compositions

The theoretical performance of ADN-based propellants was calculated using the NASA CEC-71 code. The chemical data, like molecular structure and heat of formation were obtained from ICT database. All the predictions were carried out for chemical equilibrium conditions at the chamber pressure of 7 MPa. The ratio of the nozzle exit area ( $A_e$ ) and the nozzle throat area ( $A_t$ ) values was chosen as 7. The combustion efficiency and nozzle efficiency were assumed to be 100% for all predictions. The base composition 1 with 20% AP was initially used, and

subsequently, AP was replaced by ADN in compositions 2 (AP/ADN-based) and 3 (ADN-based). The results are presented in Table 2. These findings demonstrate a significant enhancement in the energetic properties of the propellant upon the incorporation of ADN. Although ADN reduces the flame temperature of the propellant, the decrease in molecular weight of combustion products and increase in enthalpy input contribute to an overall enhancement of the specific impulse. Utilizing ADN as an oxidizer in propellants is advantageous not only for making them environmentally friendly but also for improving specific impulse.

**Table 2.** Performance comparison of propellant compositions with varying AP/ADN content using NASA CEC-71 Code

Ingredient	Composition		
	1	2	3
AP	20	10	–
ADN	–	10	20
Active binder (NBR + TEGDN)	20.62		
Quinol ether	0.35		
PbO <sub>2</sub>	0.03		
RS-RDX	41		
Aluminum powder	18		
Theoretical performance parameters			
Characteristic velocity [m·s <sup>-1</sup> ]	1627	1637.9	1649
Specific impulse, $I_{sp(70:1)}$ [s]	268.6	270.1	271.7
Oxygen balance [%]	–37.96	–38.78	–39.61
Density impulse [g·s·cm <sup>-3</sup> ]	480.8	480.23	479.55
Flame temperature [K]	3574	3565	3556
Molar weight of combustion products [g·mol <sup>-1</sup> ]	26.318	25.863	25.423
$\Delta H$ [kJ·kg <sup>-1</sup> ]	–3993.70	–3893.53	–3794.44

Based on theoretical performance predictions, compositions 1 and 3 were produced at a 500 g scale without the inclusion of hydantoin resin due to its observed incompatibility with ADN. To facilitate propellant curing in the absence of hydantoin resin, the quantities of quinol ether and PbO<sub>2</sub> were appropriately increased. The resulting cured propellant underwent sample preparation and evaluation to assess various physical, ballistic, and mechanical properties, as outlined in Table 3.

**Table 3.** Properties of AP- and ADN-based propellants

Properties	Composition 1	Composition 3
Hardness (Shore A)	50-55	30-35
Density [g/cm <sup>3</sup> ]	1.778	1.753
Theoretical maximum density, TMD [g/cm <sup>3</sup> ]	1.782	1.764
Burn rate (SSBR) at 7 MPa [mm/s]	13.50	12.80
Tensile strength at max stress [MPa]	0.64	0.24
Elongation at max stress [%]	40	26
E-mod [MPa]	1.96	0.15

It is evident from the results that the Shore A hardness of the ADN/NBR propellant is not similar to that of the base propellant. This dis-similarity indicates a deficient formation of the polymeric network due to the absence of a bonding agent. The burn rate and density values align with expectations and are comparable to those of the base propellant. However, the tensile properties highlight a significant deficiency in the cross-link behavior of the polymeric network compared to the base propellant, suggesting a notable inferiority in mechanical strength. This deficiency emphasizes the necessity for bonding agents or equivalent components to attain the required mechanical robustness.

This study underscores the advantageous energetic and environmentally friendly nature of ADN-based propellants. Nevertheless, it also emphasizes their critical shortcomings in processing and mechanical strength, which necessitate appropriate attention and resolution.

## 4 Conclusions

- ◆ ADN/NBR propellant with high performance has been successfully formulated and processed using quinol ether as curing agent, following optimal processing conditions obtained from DVS studies. DVS data highlighted the essential storage and processing requirements for ADN, suggesting storage below 25 °C at RH ≤ 50% and processing within the 35-40 °C range under controlled RH ≤ 35%.
- ◆ Though the burning rate and density (12.80 mm/s at 7 MPa and 1.753 g/cm<sup>3</sup>, respectively) of the ADN/NBR propellant are marginally different compared



to AP/NBR based propellant, thermo chemical calculations depicts the superiority of ADN/NBR propellant in terms of characteristic velocity and specific impulse.

- ◆ However, the propellant encountered compatibility issues with the bonding agent, hydantoin resin, resulting the cured propellant with inferior mechanical strength which is evident from low tensile strength, elongation and modulus.
- ◆ The application of a suitable bonding agent that provides improved mechanical properties could pave the way for its practical use. R&D efforts are ongoing in our laboratory to explore suitable bonding agent for ADN/NBR propellant to achieve good mechanical strength.

## Acknowledgements

The authors of this manuscript are very grateful to the Director, HEMRL for his valuable support and for giving us the opportunity to carry out this work.

## References

- [1] Vernacchia, M.T.; Mathesius, K.J.; Hansman, R.J. Low-Thrust Solid Rocket Motors for Small, Fast Aircraft Propulsion: Design and Development. *J. Propuls. Power* **2022**, *38*(1): 122-134; <https://doi.org/10.2514/1.B38104>.
- [2] Mason, B.P.; Roland, C.M. Solid Propellants. *Rubber Chemistry and Technology* **2019**, *92*(1): 1-24; <https://doi.org/10.5254/rct.19.80456>.
- [3] Sutton, G.P.; Biblarz, O. *Rocket Propulsion Elements*. 9<sup>th</sup> ed., John Wiley & Sons, Inc., Hoboken, New Jersey, **2017**.
- [4] DeLuca, L.T. *Chemical Rocket Propulsion*. 1<sup>st</sup> ed., (DeLuca, L.T.; Shimada, T.; Sinditskii, V.P.; Calabro, M., Eds.) Springer Cham, **2017**.
- [5] Chaturvedi, S.; Dave, P.N. Solid Propellants: AP/HTPB Composite Propellants. *Arabian J. Chem.* **2019**, *12*(8): 2061-2068; <https://doi.org/10.1016/j.arabjc.2014.12.033>.
- [6] Aziz, A.; Mamat, R.; Ali, W.K. W.; Perang, M.R.M. Review on Typical Ingredients for Ammonium Perchlorate Based Solid Propellant. *ARPJ. Eng. Appl. Sci.* **2015**, *10*(15): 6188-6191; <https://doi.org/10.4028/www.scientific.net/amm.773-774.470>.
- [7] Siglin, J.C.; Mattie, D.R.; Dodd, D.E.; Hildebrandt, P.K.; Baker, W.H. A 90-Day Drinking Water Toxicity Study in Rats of the Environmental Contaminant Ammonium Perchlorate. *Toxicol. Sci.* **2000**, *57*(1): 61-74; <https://doi.org/10.1093/toxsci/57.1.61>.
- [8] *Perchlorate Environmental Occurrence, Interactions and Treatment*. 1<sup>st</sup> ed., (Gu, B.; Coates, J.D., Eds.) Springer, New York, US-NY, **2006**; <https://doi.org/10.1007/0-387-31113-0>.
- [9] Maffini, M.V; Trasande, L.; Neltner, T. Perchlorate and Diet: Human Exposures,

- Risks, and Mitigation Strategies. *Curr. Environ. Health Rep.* **2016**, 3(2): 107-117. <https://doi.org/10.1007/s40572-016-0090-3>.
- [10] Niziński, P.; Błażewicz, A.; Kończyk, J.; Michalski, R. Perchlorate – Properties, Toxicity and Human Health Effects: An Updated Review. *Rev. Environ. Health* **2021**, 36(2): 199-222; <https://doi.org/10.1515/reveh-2020-0006>.
- [11] Li, M.; Xiao, M.; Xiao, Q.; Chen, Y.; Guo, Y.; Sun, J.; Li, R.; Li, C.; Zhu, Z.; Qiu, H.; Liu, X.; Lu, S. Perchlorate and Chlorate in Breast Milk, Infant Formulas, Baby Supplementary Food and the Implications for Infant Exposure. *Environ. Int.* **2022**, 158 paper 106939; <https://doi.org/https://doi.org/10.1016/j.envint.2021.106939>.
- [12] Medicine, P. *Wildlife Toxicity Assessment for Perchlorate*. Army Center for Health Promotion, Final Report, **2007**.
- [13] *Perchlorate in Drinking-Water Background Document for Development of WHO Guidelines for Drinking-Water Quality*. **2016**; <http://www.who.int/publications/guidelines/>.
- [14] Nagamachi, M.Y.; Oliveira, J.I.S.; Kawamoto, A.M.; de Cássia, L.; Dutra, R. ADN - The New Oxidizer around the Corner for an Environmentally Friendly Smokeless Propellant. *J. Aerosp. Technol. Manage.* **2009**, 1(2): 153-160; <https://doi.org/10.5028/jatm.2009.0102153160>.
- [15] Venkatachalam, S.; Santhosh, G.; Ninan, K.N. An Overview on the Synthetic Routes and Properties of Ammonium Dinitramide (ADN) and Other Dinitramide Salts. *Propellants, Explos., Pyrotech.* **2004**, 29(3): 178-187; <https://doi.org/10.1002/prep.200400043>.
- [16] Cannizzo, L.F.; Highsmith, T.K.; Wardle, R.B.; Campbell, C.J.; Dewey, M.A.; Bennett, R.R.; Lee, K.E.; Doll, D.W.; Mcleod, C.S.; Hajik, R.M.; Midyett, J.S. *Utilizations of Ammonium Dinitramide (ADN) in Propellant Formulations\**. **1998**.
- [17] Johansson; de Flon, J.; Pettersson, Å.; Wanhatalo, M.; Wingborg, N. Spray Prilling of ADN and Testing of ADN-Based Solid Propellants. *Proc. 3<sup>rd</sup> Int. Conf. on Green Propellants for Space Propulsion*, **2006**.
- [18] Chen, F.; Xuan, C.; Lu, Q.; Xiao, L.; Yang, J.; Hu, Y.; Zhang, G.P.; Wang, Y.; Zhao, F.; Hao, G.; Jiang, W. A Review on the High Energy Oxidizer Ammonium Dinitramide: Its Synthesis, Thermal Decomposition, Hygroscopicity, and Application in Energetic Materials. *Def. Technol.* **2023**, 19: 163-195; <https://doi.org/https://doi.org/10.1016/j.dt.2022.04.006>.
- [19] Cui, J.; Han, J.; Wang, J.; Huang, R. Study on the Crystal Structure and Hygroscopicity of Ammonium Dinitramide. *J. Chem. Eng. Data* **2010**, 55(9): 3229-3234; <https://doi.org/10.1021/je100067n>.
- [20] Santhosh, G.; Ghee Ang, H. Compatibility of Ammonium Dinitramide with Polymeric Binders Studied by Thermoanalytical Methods. *Int. J. Energ. Mater. Chem. Propul.* **2010**, 9(1): 27-41.
- [21] Iqbal, M.M.; Liang, W. Modeling the Moisture Effects of Solid Ingredients on Composite Propellant Properties. *Aerosp. Sci. Technol.* **2006**, 10(8): 695-699; <https://doi.org/https://doi.org/10.1016/j.ast.2006.07.003>.
- [22] Zeng, T.; Yang, R.; Li, D.; Li, J.; Guo, X.; Luo, P. Reactive Molecular Dynamics

- Study on the Effect of H<sub>2</sub>O on the Thermal Decomposition of Ammonium Dinitramide. *Propellants Explos., Pyrotech.* **2020**, *45*(10): 1590-1599; <https://doi.org/10.1002/prop.201900309>.
- [23] Wingborg, N. Ammonium Dinitramide–Water: Interaction and Properties. *J. Chem. Eng. Data* **2006**, *51*(5): 1582-1586; <https://doi.org/10.1021/je0600698>.
- [24] Marshall, P. V. A New Analytical Technique for Characterising the Water Vapour Sorption Properties of Powders. *Proc. Int. Symp. on Solid Oral Dosage Forms*, Stockholm, Sweden, **1994**.
- [25] Simón, C.; Fernández, F.G.; Esteban, L. G.; de Palacios, P.; Hosseinpourpia, R.; Mai, C. Comparison of the Saturated Salt and Dynamic Vapor Sorption Methods in Obtaining the Sorption Properties of *Pinus Pinea L.* *Eur. J. Wood Wood Prod.* **2017**, *75*: 919-926.
- [26] Garbalińska, H. Comparative Analysis of the Dynamic Vapor Sorption (DVS) Technique and the Traditional Method for Sorption Isotherms Determination – Exemplified at Autoclaved Aerated Concrete Samples of Four Density Classes. *Cem. Concr. Res.* **2017**, *91*: 97-105.
- [27] Wang, J.N.; Zhang, G.; Yan, R.; Hu, L.; Zhang, T. Hygroscopicity of ADN with Dynamic Method. (in Chinese) **2012**, *20*(1): 86-89; <https://doi.org/10.3969/j.issn.1006-9941.2012.01.021>.
- [28] Sheibani, N. Simulation and Experimental Study on the Incompatibility Issue between ADN and Isocyanate. *J. Mol. Model* **2022**, *28*(12) paper 405; <https://doi.org/10.1007/s00894-022-05399-y>.
- [29] Sims, S.; Fischer, S.; Tagliabue, C. ADN Solid Propellants with High Burning Rates as Booster Material for Hypersonic Applications. *Propellants Explos., Pyrotech.* **2022**, *47*(7): <https://doi.org/10.1002/prop.202200028>.
- [30] Gettwert, V.; Fischer, S. *Small Scale Motor Tests of ADN/GAP Based Propellants*.
- [31] Gettwert, V.; Franzin, A.; Manfred, B.; DeLuca, L.; Heintz, T.; Weiser, V. ADN/GAP Composite Rocket Propellants with and Without Metallic Fuels. *Int. J. Energ. Mater. Chem. Propul.* **2018**, *16*; <https://doi.org/10.1615/IntJEnergeticMaterialsChemProp.2018021254>.
- [32] Gribov, P.S.; Kondakova, N.N.; Il'icheva, N.N.; Stepanova, E.R.; Denisyuk, A.P.; Sizov, V.A.; Dotsenko, V.D.; Vinogradov, D.B.; Bulatov, P.V.; Sinditskii, V.P.; Suponitsky, K.Y.; Il'in, M.M.; Keshtov, M.L.; Sheremetev, A.B. Energetic Polymer Possessing Furazan, 1,2,3-Triazole, and Nitramine Subunits. *Int. J. Mol. Sci.* **2023**, *24*(11): <https://doi.org/10.3390/ijms24119645>.
- [33] Klyuchnikov, O.R.; Deberdeev, R.Ya.; Zaikov, G.E. Low-Temperature Vulcanisation of Unsaturated Rubbers by C-Nitroso Systems. *International Polymer Science and Technology* **2006**, *33*(8): 51-56; <https://doi.org/10.1177/0307174X0603300810>.
- [34] Singh, S.; Raveendran, S.; Kshirsagar, D.R.; Gupta, M.; Bhongale, C.J. Studies on Curing of an Aluminized Ammonium Perchlorate Composite Propellant Based on Nitrile Butadiene Rubber Using a Quinol Ether of 1,4-Benzoquinone Dioxime. *Cent. Eur. J. Energ. Mater.* **2022**, *19*(1): 18-38; <https://doi.org/10.22211/cejem/147553>.

- [35] *Chemical Compatibility of Ammunition Components with Explosives (Non Nuclear Applications)*. STANAG 4147 - Ed: 2, **2001**.
- [36] Agrawal, J.P. Salient Features of Explosives. In: *High Energy Materials*. **2010**, pp. 1-67; <https://doi.org/https://doi.org/10.1002/9783527628803.ch1>.
- [37] Gan, J.; Zhang, X.; Zhang, W.; Hang, R.; Xie, W.; Liu, Y.; Luo, W.; Chen, Y. Research Progress of Bonding Agents and Their Performance Evaluation Methods. *Molecules* **2022**, *27*(2) paper 340; <https://doi.org/10.3390/molecules27020340>.

## Contribution

Kavita Ghosh:	conception, foundations, methods, performing the experimental part
Deepak Yadav:	conception, foundations, methods, performing the experimental part
Vaibhav Sadavarte:	conception, foundations, performing the experimental part
Lalita Jawale:	performing the experimental part
Rajesh BabanRao Pawar:	other contribution to the publication
Ramesh Kurva:	other contribution to the publication

Received: August 2, 2024

Revised: September 26, 2024

First published online: September 30, 2024